JOURNAL OF MATERIALS SCIENCE 21 (1986) 75–82

Surface structures produced in 1C–1.5Cr and 0.38C–Ni–Cr–Mo steels by high-power CO_2 laser processing

M. CARBUCICCHIO
Department of Physics, University of Parma, Parma, Italy
G. PALOMBARINI
Institute of Metallurgy, University of Bologna, Bologna, Italy

The effects of surface high-power laser processing were studied for 1C–1.5Cr and 0.38C–Ni–Cr–Mo steels by changing the incident power density and laser–material interaction time. Both melted and solid-state transformed regions were produced, and studied by means of depth-selective surface Mössbauer measurements, X-ray diffraction analyses, metallography and microhardness measurements. The results are compared with those previously obtained by laser surface-melting of 0.4C carbon steel, and are discussed with reference to the carbon content in the base alloys as well as the conditions of laser processing.

1. Introduction

Treating the surfaces of metals and alloys with high-power lasers allows peculiar modifications of the microstructures to be obtained. Laser treatments, in fact, can produce very sharp thermal gradients in extremely short periods of time. In particular, increasing attention is being given to processes of rapid surface-melting and quenching.

A knowledge of the basic phenomena occurring during surface melting and subsequent cooling is essential to develop surface alloying, cladding and rapid solidification surface treatments. In the important field of laser surface-melting of ferrous alloys, some general features of the melted zones have been pointed out with regard to steels and cast irons. Trafford *et al.* [1] treated a 2.9 to 3.2 wt % C grey cast iron containing 1.7 to 2.1% Si and 0.5 to 0.8% Mn with a 5 kW CO_2 laser, under conditions allowing treated layers to be obtained with and without surface melting. The surface-melted alloy displayed significant increases in surface hardness and resistance to abrasive wear [1]. Blarasin *et al.* [2] also obtained a considerable improvement in hardness and wear resistance for a grey cast iron, laser melted to 0.5 to 0.7 mm in depth. Christodoulou *et al.* [3] investigated the effects of different surface coating conditions on the microstructure of surface melted zones produced on alloy steels. For the 1C–1.4Cr steel, the resulting structures were either essentially martensitic with retained austenite or mainly austenitic with small amounts of irregularly-distributed martensite. The effects of rapid solidification on the microstructures of laser-processed molybdenum and chromium steels were studied by Molian [4] and by Molian and Wood [5]. The phase transformations, as well as composition and morphology of phases, particularly carbides, were correlated with the base alloy composition with the aid of scanning and transmission electron microscopy [4, 5].

In the present work, c.w.-CO_2 high-power laser treatments were carried out on a 1C–1.5Cr steel and a low-alloy 0.38C–Ni–Cr–Mo steel, under conditions of incident power and interaction time which generally were sufficient to melt surface layers of different thicknesses. The aim was to investigate both the effects of different laser conditions on the same alloy, and the effects of the same laser treatment on differently-alloyed steels.

2. Experimental details

Plates 10 mm thick of a 1C–1.5Cr steel and a 0.38C–Ni–Cr–Mo steel, whose composition is reported in Table I, were coated with an anti-reflection film of graphite and then subjected to single-pass laser treatments in air, using a c.w.-CO_2 high-power laser source. The following treatments were used: 5.4 and 11.6 kW cm^{-2} incident power densities, and 4.5, 1.66 and 0.78 m min^{-1} beam translation speeds. The sizes of the laser spot were 10 mm × 10 mm and, therefore, the beam–material interaction times were 0.13. 0.36 and 0.77 sec respectively.

The laser-treated regions were studied by means of X-ray diffraction and surface Mössbauer measurements. The X-ray diffraction analyses were carried out using a computer-controlled goniometer and Co$K\alpha$ radiation. The Mössbauer measurements were performed at room temperature, using the experimental technique described elsewhere [6], by detecting the K X-ray (6.4 keV) and K-shell conversion electrons (7.3 keV) resonantly re-emitted by the ^{57}Fe atoms. The Mössbauer X-ray measurements allowed surface layers $\sim 25\,\mu$m thick to be analysed. Surface regions of different thicknesses down to a maximum depth of 220 nm were analysed by selecting in the 5.4 to 7.3 keV

0022–2461/86 $03.00 + .12

TABLE I Compositions of steels

Steel	Element (wt %)							
	C	Si	Mn	P	S	Cr	Mo	Ni
1C–1.5Cr	1.00	0.28	0.38	0.009	0.014	1.48	–	–
0.38C–Ni–Cr–Mo	0.38	0.33	0.62	0.002	0.024	0.84	0.15	0.79

range the energy of the conversion electrons emerging from the surface. The depths of analysis were estimated according to Krakowski and Miller [7], with a correction for the escape of detected radiation from different phases [8]. The spectra were computer-fitted to a set of Lorentzian peaks.

Cross-sections of the treated plates were prepared for metallography and microhardness measurements. A Vickers indenter was used, with a 1 N load.

3. Results and discussion

3.1. 1C–1.5Cr steel treated at 5.4 kW cm^{-2}

For beam translation speeds ranging from 4.50 to 0.78 m min^{-1}, all the samples underwent surface melting. By increasing the interaction time from 0.13 to 0.77 sec, the depths of the melted zones increased from $\sim 60\,\mu$m to $\sim 190\,\mu$m, while the depth of the thermally affected zones increased from $\sim 615\,\mu$m to $\sim 1250\,\mu$m.

Generally, the melted and rapidly solidified zones showed polyphasic structures, with predominantly dendritic morphologies. For the samples treated at 4.5 m min^{-1}, the underlying solid-state transformed regions were constituted by a distinct upper white and relatively soft layer (HV $\simeq$ 4.2 kN mm^{-2}), and a lower coarse martensite layer containing lightly-etching regions attributable to retained austenite (Fig. 1). At higher resolution, obtained by means of a strongly-tapered metallographic section, the white layer displays a microstructure of equiaxial grains containing a darker phase segregated at the grain boundaries and irregularly-distributed coarse crystals of martensite. In the case of a morphologically-similar white layer, previously observed on a laser surface-melted medium carbon steel, the large-grained phase was identified as austenite with cementite at the grain boundaries [9].

As the translation speed of the beam decreased (1.66 and 0.78 m min^{-1}) at constant incident power, the distinct white layer progressively disappeared in the solid-state transformed regions and the microstructures observed were similar to those obtained by Christodoulou *et al.* [3] on a graphite-coated 1C–1.4Cr steel, surface-melted at 1.7 kW with a 1 mm mean diameter and 135 mm sec^{-1} translation speed.

The structural heterogeneities observed in both the solidified and solid-state transformed regions are the cause of very large fluctuations in the values of microhardness (Fig. 2).

Because of the considerable depths of melting, both the X-ray diffraction and Mössbauer measurements on the as-treated samples concern the outer part of the melted zones. Fig. 3a shows the X-ray diffraction pattern for the sample treated at 1.66 m min^{-1}. This pattern is due to austenite, cementite and to another phase that, with support from the metallographic analysis, can be interpreted as being martensite.

For the same sample, a careful analysis of the most external, melted and rapidly cooled regions was made possible by conversion-electron Mössbauer measurements. The Mössbauer spectra reported in Figs. 4a and b were obtained by selecting the conversion electrons in the 6.5 to 7.3 and the 5.5 to 6.5 keV energy ranges. The corresponding depths of analysis were evaluated as 0 to ~ 100 nm and ~ 100 to ~ 200 nm, respectively. Both the spectra can be interpreted as the superimposition of several spectra:

Spectrum I: a central peak and a quadrupole doublet, due to paramagnetic austenite;

Spectrum II: a broad quadrupole doublet, which can be interpreted as due to small particles of iron oxide showing a superparamagnetic behaviour;

Spectrum III: a six-line spectrum, due to cementite;

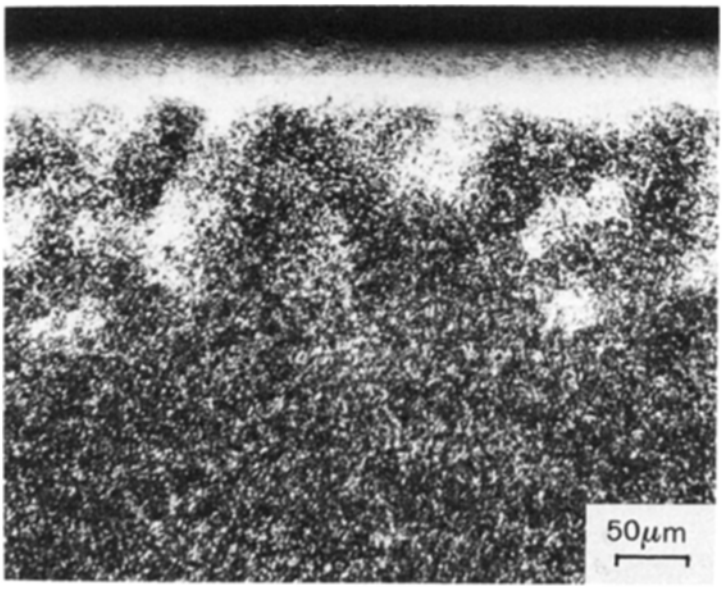

Figure 1 Metallographic cross-section of a 1C–1.5Cr steel, laser-treated at 5.4 kW cm^{-2} and 4.5 m min^{-1}.

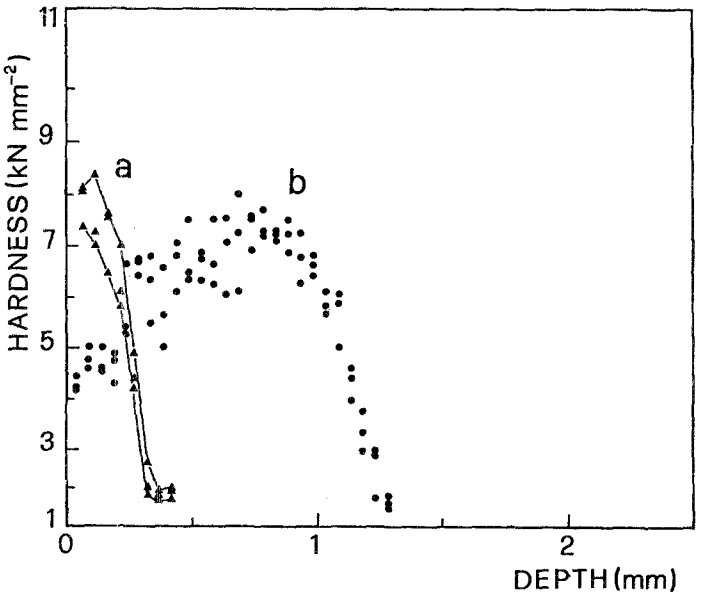

Figure 2 Hardness profiles measured through the laser-transformed regions, normal to the external surface, for the 1C–1.5Cr steel, laser- treated at 5.4 kW cm^{-2}: (a) 4.5 and (b) 0.78 m min^{-1}.

Spectrum IV: a multicomponent ferromagnetic spectrum, which can be attributed to martensite;

Spectrum V: another ferromagnetic spectrum due to iron atoms in Fe_3O_4; and

Spectrum VI: a six-line spectrum, due to iron atoms in α-Fe_2O_3.

A broadening of most Mössbauer lines can be ascribed to the presence of slightly-distorted iron sites. The formation of small particles of iron oxide, as well as the probable growth of phases with slightly-distorted iron sites, can be explained by considering the particularly heavy conditions of the thermal treatments. It should be noted that a phase identified as ferrite has been found close to the external surface of melted zones produced on a medium carbon steel [9].

With regard to the relative amounts of different phases, from area measurements of the contributions to the surface Mössbauer spectra it can be deduced that, on going towards the external surface of the melted zone, austenite decreases while martensite increases. It is to be noted that this effect holds also at higher depths, as shown by 6.4 keV X-ray Mössbauer measurements carried out on the same sample (Fig. 4c). In agreement, X-ray diffraction patterns measured on this sample abraded layer by layer showed an increasing contribution from austenite.

As regards iron oxides, the surface analysis (Figs. 4a and b) indicates an outward concentration of α-Fe_2O_3 and an inward concentration of Fe_3O_4. Moreover, the iron oxides are confined to the external surface of the laser-melted zones. In fact, iron oxides do not contribute to the X-ray Mössbauer spectrum (Fig. 4c), nor to the X-ray diffraction pattern (Fig. 3a), while they do contribute to the conversion-electron Mössbauer spectra (Figs 4a and b). A similar situation has been found for relatively thin laser-melted zones produced on a 0.4 wt % C carbon steel [9].

At a higher interaction time (0.77 sec), the iron oxides Fe_3O_4 and α-Fe_2O_3 contribute to the X-ray diffraction pattern (Fig. 3b), as well as to the 6.4 keV X-ray Mössbauer spectrum.

The formation of surface iron oxides proves that strong melt–environment interactions can occur, notwithstanding the presence of the anti-reflection graphite coating. The extent of oxidation increases with increasing interaction time. Reasonably, these melt-

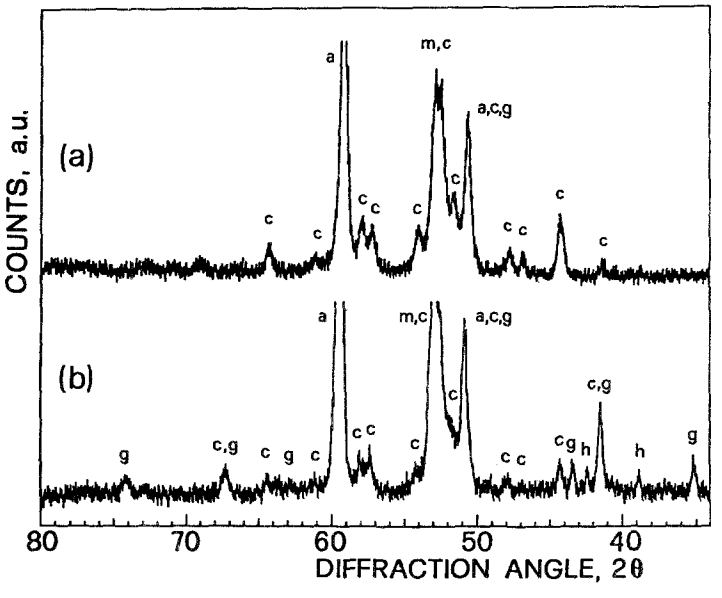

Figure 3 X-ray diffraction patterns of the 1C–1.5Cr steel, laser-treated at 5.4 kW cm^{-2}: (a) 1.66 and (b) 0.78 m min^{-1}. Letters a, c, m, g and h mean austenite, cementite, martensite, Fe_3O_4 and α-Fe_2O_3, respectively.

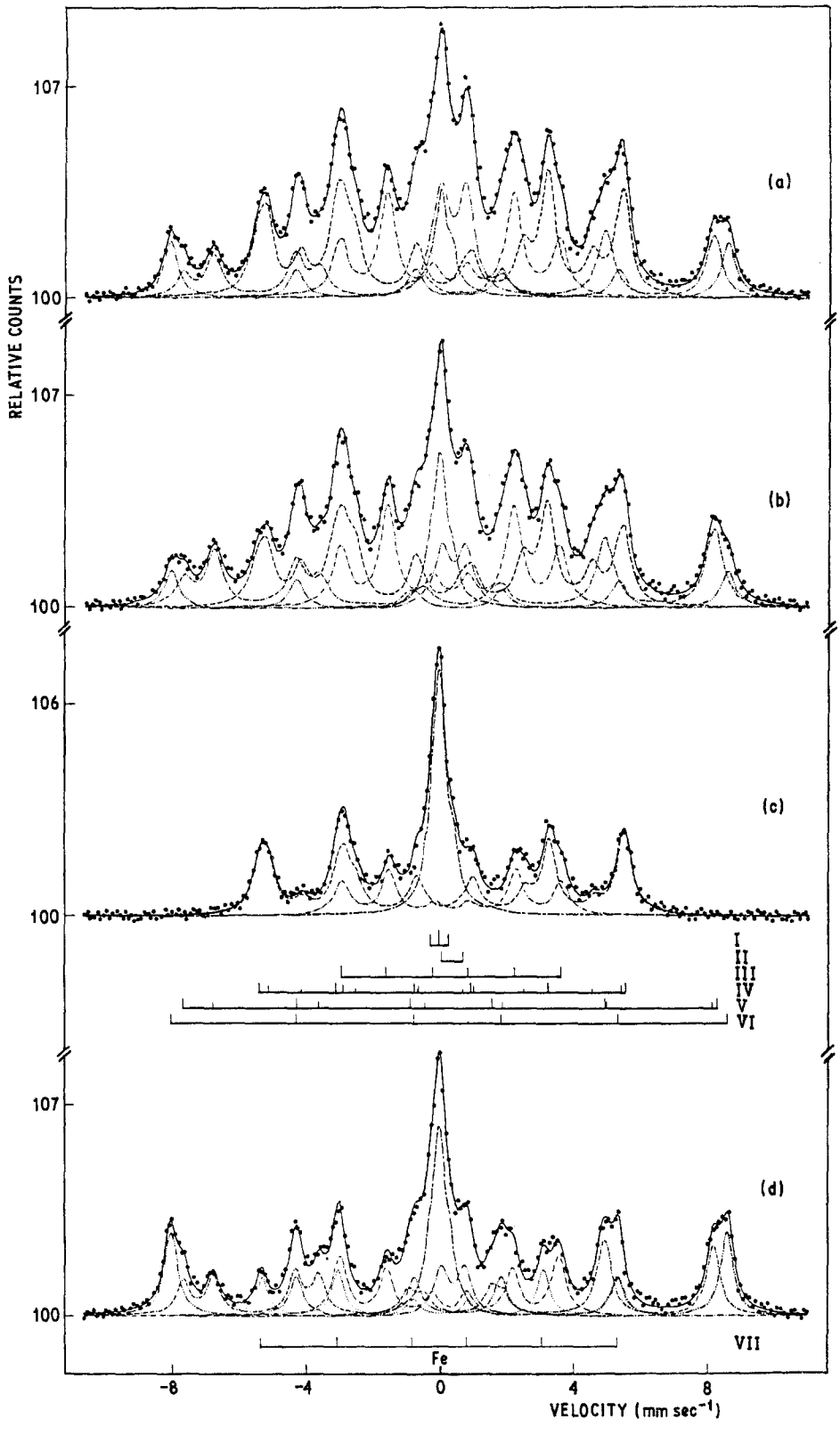

Figure 4 Room-temperature surface Mössbauer spectra. (a) to (c) 1C–1.5rCr steel, laser-treated at 5.4 kW cm^{-2} and 1.66 m min^{-1}: (a) 6.5 to 7.3 keV conversion electrons, (b) 5.5 to 6.5 keV conversion electrons, (c) 6.4 keV X-rays. (d) 0.38C–Ni–Cr–Mo steel treated at 11.6 kW cm^{-2} and 4.5 m min^{-1}, 6 to 7.3 keV conversion electrons.

environment interactions also lead to decarburizing effects; the corresponding losses of carbon can be related to the observed decrease of austenite towards the external surface of the melted zones. These results support a stabilizing effect of carbon on austenite [3, 9], rather than a nucleating effect of oxide particles on martensite [10].

3.2. 1C–1.5Cr steel treated at 11.6 kW cm^{-2}

With decreasing beam translation speeds from 4.5 to 0.78 m min^{-1}, the melting depth increased from ~65 to ~940 μm, while the depth of the thermally affected zone increased from ~650 to ~2460 μm. The general features of the laser-transformed regions resembled those observed for samples of the same steel treated at 5.4 kW cm^{-2}. In particular, (i) the solidified zones had polyphasic structures and dendritic morphologies, and (ii) the solid-state transformed zones contained martensite with retained austenite, with an upper mainly austenitic white layer which gradually

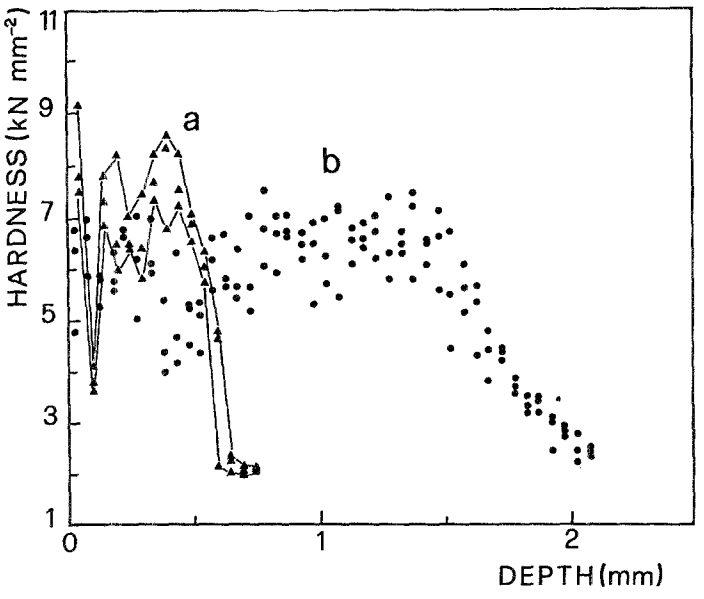

Figure 5 Hardness profiles measured as reported in Fig. 2, for the 1C–1.5Cr steel, laser-treated at 11.6 kW cm^{-2}: (a) 4.5 and (b) 0.78 m min^{-1}.

disappeared as the beam translation speed was decreased. Reported in Fig. 5 are microhardness profiles of these samples, showing large fluctuations due to microstructural heterogeneities.

For the sample treated at 0.78 m min^{-1}, the metallographic observations of the solid-state transformed region showed an upper zone containing large amounts of spheroidal carbide particles in a matrix of coarse martensite with retained austenite (Fig. 6). This may well be the consequence of the particularly high volume and thermal capacity of the outer melted region.

When the beam translation speed was decreased, the amounts of cementite were found to decrease in the melted zones, while the amounts of iron oxides increased at the external surfaces (Fig. 7). This may well be due to particularly strong melt–environment interactions. Moreover, the lower proportion of austenite formed at higher interaction times can be ascribed to the extent of these interactions, and this lends further support to the important role of carbon in stabilizing austenite.

3.3. 0.38C–Ni–Cr–Mo steel treated at 5.4 kW cm^{-2}

At a beam translation speed of 4.5 m min^{-1}, the steel only underwent a solid-state transformation, leading to a structure of coarse martensite with some retained austenite. The corresponding X-ray diffraction pattern is shown in Fig. 8a. The thermally affected zone was $\sim 80\,\mu$m deep. The samples treated at 0.78 and 1.66 m min^{-1} underwent surface melting, down to $\sim 40\,\mu$m in depth, with thermally affected zones reaching $\sim 170\,\mu$m. These depths are considerably lower than those found for the 1C–1.5Cr steel treated under the same processing conditions. The lower depths of melting found for the low-alloy steel can be explained by considering that the treated alloys differ considerably in carbon content, which in turn can determine different melting behaviours.

The general features of the melted zones were similar to those obtained for the 1C–1.5Cr steel. These zones contained mainly austenite and cementite as well as, on the external surfaces, Fe_3O_4 and α-Fe_2O_3 in amounts which depend on the laser processing

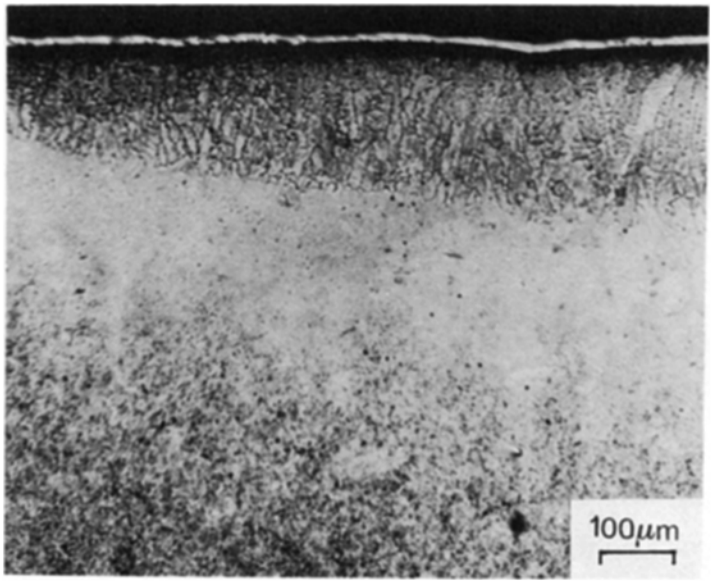

Figure 6 Metallographic cross-section of a 1C–1.5Cr steel, laser-treated at 11.6 kW cm^{-2} and 0.78 m min^{-1}.

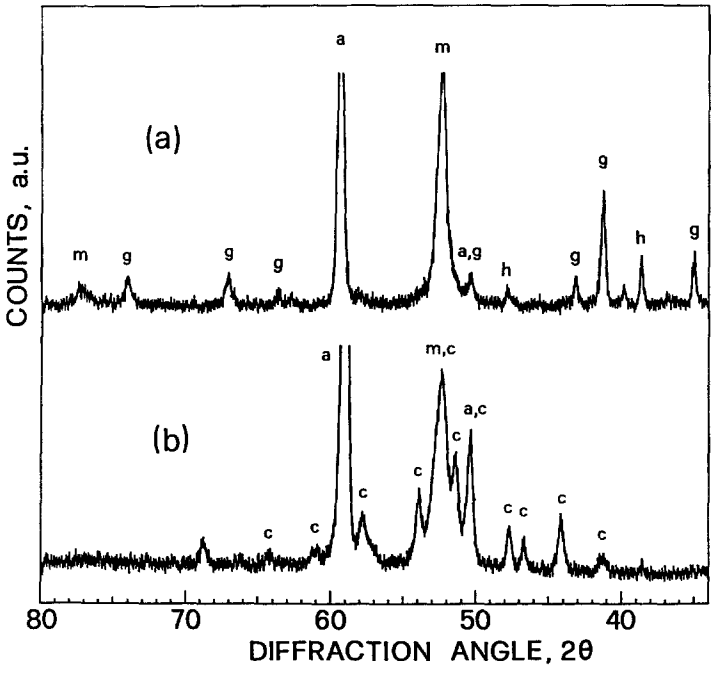

Figure 7 X-ray diffraction patterns of the 1C–1.5Cr steel, laser-treated at 11.6 kW cm^{-2}: (a) 0.78 and (b) 4.5 m min^{-1}. Letters a, c, m, g and h mean austenite, cementite, martensite, Fe_3O_4 and α-Fe_2O_3, respectively.

conditions. Moreover, there were some indications of the presence of both martensite and ferrite, No similar indications were found in the case of 1C–1.5Cr steel. With regard to this problem, better experimental evidence was found for the 0.38C–Ni–Cr–Mo steel treated at 11.6 kW cm^{-2} and, therefore, this point will be discussed in the next section.

In all the samples subjected to surface melting, the solid-state transformed regions were constituted by an upper mainly austenitic white layer, and an underlying region of coarse martensite with large amounts of retained austenite (Fig. 9); microstructural heterogeneities in these samples are reflected in the corresponding hardness profiles (Fig. 10). In comparison, in the case of the 1C–1.5Cr steel the white layers were found only beneath zones that had undergone little melting (Fig. 1). This difference between the two steels can be correlated with the differences in melting depth, as well as the different chemical compositions. A lower volume and, therefore, a lower thermal capacity of the melted zone, in fact, induces steeper thermal gradients in the underlying solid material.

3.4. 0.38C–Ni–Cr–Mo steel treated at 11.6 kW cm^{-2}

All the samples treated in the range 4.5 to 0.78 m min^{-1} beam translation speed underwent surface melting, down to a maximum depth of $\sim 300\mu$m. The thermally affected zones, in turn, reached $\sim 2500\,\mu$m. The structure and phase composition of both the solidified and solid-state transformed regions were substantially similar to those observed for the samples surface-melted at 5.4 kW cm^{-2}. In the case of samples treated at 4.5 m min^{-1}, iron oxides were found to contribute only to conversion-electron Mössbauer spectra (Fig. 4d). Hardness profile of the laser-treated zones are shown in Fig. 11. As regards melt volumes and white layer formation, the remarkable differences found between the two steels treated at 11.6 kW cm^{-2} can be explained in the same way as for the case of the same materials treated at 5.4 kW cm^{-2}.

Another difference between the two steels concerns the presence of ferrite in the outer parts of the melted zones produced on the 0.38C–Ni–Cr–Mo steel. The conversion-electron Mössbauer spectrum measured for

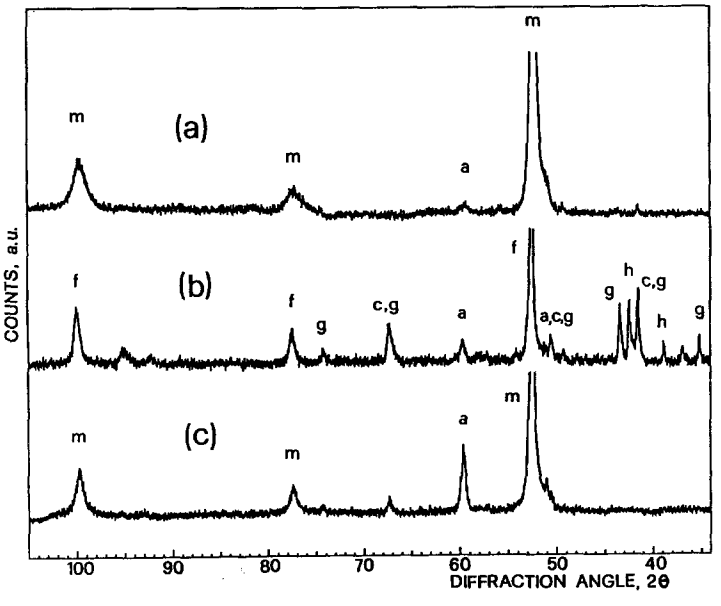

Figure 8 X-ray diffraction patterns of the laser-treated 0.38C–Ni–Cr–Mo steel: (a) 5.4 kW cm^{-2}, 4.5 m min^{-1} (no surface melting); (b) 11.6 kW cm^{-2}, 0.78 m min^{-1}; (c) same sample as in (b), after abrasion of a $\sim 20\,\mu$m thick surface layer. Letter f means ferrite.

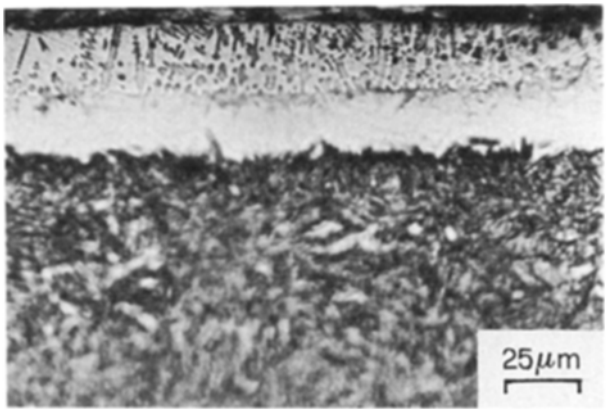

Figure 9 Metallographic cross-section of a 0.38C–Ni–Cr–Mo steel, laser-treated at 5.4 kW cm^{-2} and 0.78 m min^{-1}.

the low-alloy steel, in fact, shows a contribition from Spectrum VII (Fig. 4d), instead of the Spectrum IV found in similar spectra measured for the 1C–1.5Cr steel (Figs. 4a and b). Spectrum VII is due to iron atoms in environments such as in pure b c c iron and, therefore, can be interpreted as due to ferrite. At higher depths in the same sample, the presence of martensite is shown both by the 6.4 keV X-ray Mössbauer spectrum and by the X-ray diffraction pattern.

When the laser beam translation speed is decreased, the amount of ferrite in the outer part of the melted zones increases considerably. In fact, ferrite contributes to the X-ray diffraction pattern relative to the as-treated sample (Fig. 8b), while martensite mainly contributes to the pattern measured for the same sample after abrasion of a $\sim 20\,\mu$m thick surface layer (Fig. 8c). The formation of ferrite in the outer parts of melted zones can be attributed to the relatively low cooling rates of these parts, as well as to decarburizing effects whose occurrence is suggested by the growth of iron oxides. Also taking into account the fact that both the composition and thermal conditions of the laser-melted zones can locally undergo considerable heterogeneities, the local transformation of austenite into ferrite and cementite in the 0.38C–Ni–Cr–Mo steel can be ascribed to the relatively slow cooling of solidified low-carbon austenitic areas whose amounts, in a medium-carbon steel, may be relatively high.

4. Conclusions

The c.w.-CO_2 power-laser treatments carried out on graphite-coated 1C–1.5Cr and 0.38C–Ni–Cr–Mo steels under processing conditions which were suitable for obtaining surface melting allow the following conclusions to be drawn:

1. Under the same conditions of treatment, the melting depths were considerably higher for the high-carbon steel. In particular, at 5.4 kW cm^{-2} incident power density and 4.5 m min^{-1} beam translation speed, the medium-carbon steel only underwent solid-state transformation.

2. Generally, the melted zones had polyphasic structures and dendritic morphologies, and where constituted mainly by austenite, cementite and martensite. Notwithstanding the presence of the anti-reflection graphite coating, melt–environment interactions occurred giving rise to surface iron oxides, in amounts depending on the laser processing conditions.

3. Lower proportions of austenite are concomitant with larger amounts of iron oxides, as shown both by surface and depth-selective analyses carried out on samples treated under very different processing conditions. This supports the important role of carbon in stabilizing austenite.

4. Appreciable amounts of ferrite can form in the outer parts of melted zones produced on medium-carbon steels, due to the concurrent action of relatively low cooling rates and decarburizing melt–environment interactions. In the case of the 1C–1.5Cr steel, ferrite formation is hindered by the high carbon content.

5. The solid-state transformed regions are constituted mainly by coarse martensite and different amounts of retained austenite. Moreover, soft upper layers of large-grained austenite, with intergranular cementite and irregularly-distributed martensite, can form depending on the chemical composition of the treated alloy and the melted volume.

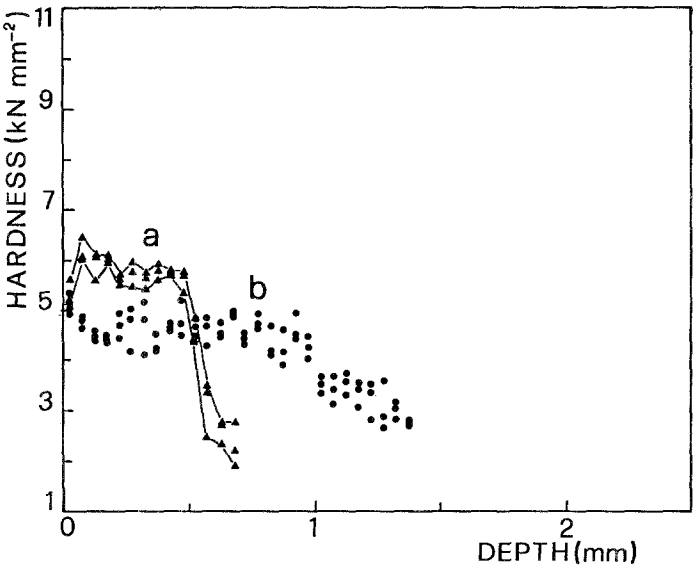

Figure 10 Hardness profiles measured as reported in Fig. 2, for the 0.38C–Ni–Cr–Mo steel, laser-treated at 5.4 kW cm^{-2}: (a) 1.66 and (b) 0.78 m min^{-1}.

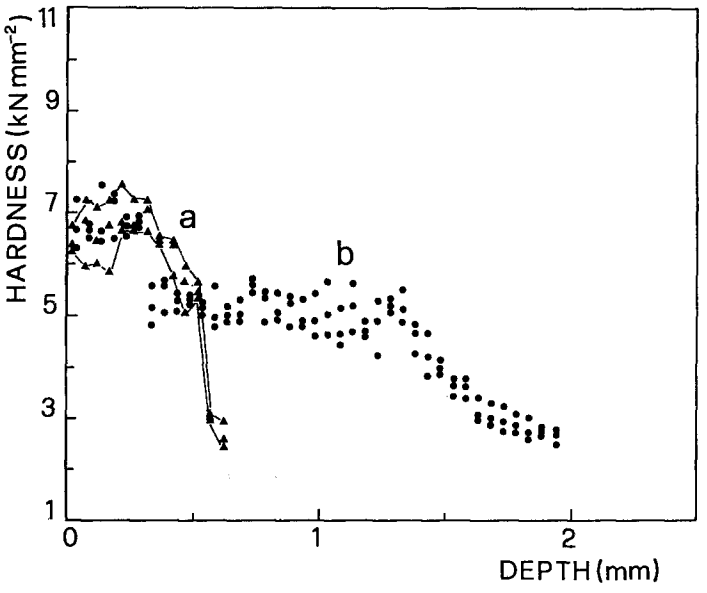

Figure 11 Hardness profiles measured as reported in Fig. 2, for the 0.38C–Ni–Cr–Mo steel, laser-treated at 11.6 kW cm^{-2}: (a) 4.5 and (b) 0.78 m min^{-1}.

6. The laser-treated zones generally show microstructural heterogeneities, which are responsible for large fluctuations in hardness properties. Therefore, further experimental work is required to optimize the laser processing conditions.

Acknowledgments

The authors wish to thank the RTM Institute, Vico Canavese, Torino, Italy for making available the facilities of its 15 kW AVCO laser. The authors also thank Professors G. Poli and G. Sambogna, University of Bologna, for help and advice. This work was carried out with financial support from CNR, Roma, under the "Progetto Finalizzato Laser di Potenza" and the "Progetto Finalizzato Metallurgia".

References

1. D. N. H. TRAFFORD, T. BELL, J. H. P. C. MEGAW and A. S. BRANDSEN, *Met. Technol.* **10** (1983) 69.
2. A. BLARASIN, S. CORCORUTO, A. BELMONDO and D. BACCI, *Wear* **86** (1983) 315.
3. G. CHRISTODOULOU, A. WALKER, W. M. STEEN and D. R. F. WEST, *Met. Technol.* **10** (1983) 215.
4. P. A. MOLIAN, *Mater. Sci. Eng.* **58** (1983) 175.
5. P. A. MOLIAN and W. E. WOOD, *ibid.* **62** (1984) 271.
6. M. CARBUCICCHIO, *Nucl. Instrum. Meth.* **144** (1977) 225.
7. R. A. KRAKOWSKI and R. B. MILLER, *ibid.* **100** (1972) 93.
8. V. E. COSSLETT and R. N. THOMAS, *Br. J. Appl. Phys.* **15** (1964) 883.
9. M. CARBUCICCHIO, G. MEAZZA, G. PALOMBARINI and G. SAMBOGNA, *J. Mater. Sci.* **18** (1983) 1543.
10. B. G. LEWIS, D. A. GILBERT and P. R. STRUTT, "Lasers in Metallurgy", edited by H. Mukherjee and J. Mazumder (Metallurgical Society of AIME, New York, 1981) p. 33.

Received 16 November 1984
and accepted 28 February 1985